ORIGINAL ARTICLE

Integrated metabolomics reveals altered lipid metabolism in adipose tissue in a model of extreme longevity

Justin Darcy · Yimin Fang · Samuel McFadden · Matthew D. Lynes · Luiz O. Leiria ·
Jonathan M. Dreyfuss · Valerie Bussburg · Vladimir Tolstikov · Bennett Greenwood ·
Niven R. Narain · Michael A. Kiebish · Andrzej Bartke · Yu-Hua Tseng

Abstract Adipose tissue plays an essential role in metabolic health. Ames dwarf mice are exceptionally long-lived and display metabolically beneficial phenotypes in their adipose tissue, providing an ideal model for studying the intersection between adipose tissue and longevity. To this end, we assessed the metabolome and lipidome of adipose tissue in Ames dwarf mice. We observed distinct lipid profiles in brown versus white adipose tissue of Ames dwarf mice that are consistent with increased thermogenesis and insulin sensitivity, such as increased cardiolipin and decreased ceramide concentrations. Moreover, we identified 5-hydroxyeicosapentaenoic acid (5-HEPE), an ω-3 fatty acid metabolite, to be increased in Ames dwarf brown adipose tissue (BAT), as well as in circulation. Importantly, 5-HEPE is increased in other models of BAT activation and is negatively correlated with body weight, insulin resistance, and circulating triglyceride concentrations in humans. Together, these data represent a novel lipid signature of adipose tissue in a mouse model of extreme longevity.

J. Darcy · M. D. Lynes · L. O. Leiria · Y.-H. Tseng
Joslin Diabetes Center, Section on Integrative Physiology and Metabolism, Harvard Medical School, Boston, MA, USA

Y. Fang · S. McFadden · A. Bartke
Department of Internal Medicine, Geriatric Research, Southern Illinois University School of Medicine, Springfield, IL, USA

L. O. Leiria
Center for Research in Inflammatory Diseases (CRID), Department of Pharmacology, Ribeirão Preto Medical School, University of São Paulo, Ribeirão Preto, SP, Brazil

J. M. Dreyfuss
Bioinformatics and Biostatistics Core, Joslin Diabetes Center, Harvard Medical School, Boston, MA, USA

V. Bussburg · V. Tolstikov · B. Greenwood · N. R. Narain · M. A. Kiebish
BERG, Framingham, MA, USA

Y.-H. Tseng (✉)
Harvard Stem Cell Institute, Harvard University, Cambridge, MA, USA
e-mail: Yu-Hua.Tseng@joslin.harvard.edu

Introduction

Brown and white adipose tissue in health and aging

Although medical advances in the twentieth and twenty-first centuries have had profound effects on extending lifespan, healthspan has unfortunately remained relatively unchanged. This inconsistency has placed a large socioeconomic burden on developed nations that continue to see a rise in age-related diseases such as type 2 diabetes, dementias, and cancers, which together account for the majority of healthcare costs and resources

(Goldman et al. 2013; Kirkland 2016). Indeed, impaired metabolism and obesity are major risk factors for many age-related diseases. Unfortunately, obesity and insulin resistance affect nearly a quarter of adults (Blackburn and Walker 2005), and their prevalence continues to increase worldwide. Therefore, therapeutic strategies that can target aging, obesity, and metabolic dysfunction are urgently needed.

Adipose tissue plays an important role in health and aging. In mammals, distinct types of adipose tissue have different functions. White adipose tissue (WAT) is the major site of energy storage, whereas brown adipose tissue (BAT) and the related beige adipose tissue specialize in thermogenic energy expenditure (Ikeda et al. 2018; Lynes and Tseng 2018; Oguri and Kajimura 2020). In addition to their roles in energy metabolism, both WAT and BAT also act as major endocrine/paracrine organs by secreting adipokines that regulate nutrient metabolism and insulin sensitivity. WAT stores calories during caloric excess and readily provides fatty acids as fuel during conditions of negative energy balance. However, dysfunction of WAT can lead to chronic inflammation during aging and obesity through the secretion of pro-inflammatory cytokines, some of which originate from an increase in resident senescent cells (Khosla et al. 2020). This, in turn, leads to insulin resistance (Zhu et al. 2014). The rediscovery of BAT in adult humans just over a decade ago (Cypess et al. 2009; Nedergaard et al. 2007; Saito et al. 2009; van Marken Lichtenbelt et al. 2009; Virtanen et al. 2009; Zingaretti et al. 2009) spurred an ever-increasing amount of research directed at the use of BAT as a potential therapeutic target to treat the growing obesity and diabetes epidemics (Chen et al. 2019; Kajimura et al. 2015; Nedergaard and Cannon 2010; Schrauwen et al. 2015). Brown and its related beige adipose tissues are excellent targets to combat obesity owing to their capability of dissipating energy through the action of uncoupling protein 1, which dissociates the electron transport chain from ATP production. To maintain thermogenic output by converting chemical energy into heat, BAT acts as a "metabolic sink" and consumes circulating fuel substrates for catabolism. Beyond energy expenditure and consumption of macromolecules, BAT has beneficial effects through its secretory function (Villarroya et al. 2017). Indeed, we and others have identified secreted lipids that act as signaling molecules, and are capable of influencing glucose and lipid metabolism (Leiria et al. 2019; Lynes et al. 2017).

Importantly, many of these beneficial effects of BAT activation overlap with improved metabolic aging (Darcy and Tseng 2019). Since BAT activity decreases with age, particularly in the post-menopause and post-andropause life stages where age-related diseases begin to occur (Cypess et al. 2009; Mancuso and Bouchard 2019), there is the possibility that activating BAT may not only combat age-related obesity but also increase metabolic healthspan.

Characteristics of long-lived Ames dwarf mice

Ames dwarf mice have a *Prophet of pituitary factor 1* (*Prop1*) deficiency, which results in a lack of differentiation of somatotrophs, lactotrophs, and thyrotrophs during embryonic development. This, in turn, leads to a deficiency in growth hormone (GH), thyroid-stimulating hormone, prolactin, and their downstream hormones. Importantly, Ames dwarf mice live about 50% longer than their control littermates (Brown-Borg et al. 1996). Moreover, Ames dwarf mice have an extended metabolic healthspan (Aguiar-Oliveira and Bartke 2019), which may be partially due to altered adipose tissue function. Indeed, Ames dwarf mice have increased BAT activity (Darcy and Bartke 2017; Darcy et al. 2018; Darcy et al. 2016), which plays a major role in their improved energy metabolism (Westbrook et al. 2014). Along with increased BAT activity, Ames dwarf mice have other favorable phenotypes in their WAT, including a switch from pro- to anti-inflammatory cytokine production (e.g., increased adiponectin and decreased TNF-α production) (Wang et al. 2006), improved preadipocyte adipogenic differentiation capacity in late life (Stout et al. 2014), improved insulin sensitivity (Wiesenborn et al. 2014), and increased rate of glucose disposal (Wiesenborn et al. 2014). Moreover, the closely related Snell dwarf mouse has a delay in preadipocyte senescence (Stout et al. 2014). Indeed, many adipose tissue phenotypes may underlie the resistance to metabolic syndrome observed in Ames dwarf mice exposed to a high-fat diet, despite the fact that they become obese (Hill et al. 2016).

Modern techniques in the field of adipocyte biology

Just as microarray and RNA sequencing have allowed researchers to gain new insights into transcriptomics, highly sensitive omic approaches such as metabolomics, proteomics, and lipidomics have transformed

workflows of metabolic researchers. In the field of adipocyte biology, these types of unbiased analyses have been done to distinguish key differences in lipid molecular species composition between BAT and WAT (Hoene et al. 2014), examine cold-induced lipid remodeling in thermogenic adipose tissue (Lynes et al. 2018), and determine exercise-specific lipid remodeling in adipose tissue (May et al. 2017). However, these critical techniques are minimally used in the context of aging in specific metabolic tissues. Indeed, most of these approaches are used to examine circulating lipids and metabolites (Gonzalez-Covarrubias et al. 2013; Lewis et al. 2018; Viltard et al. 2019), which reflect whole-body alterations rather than critical alterations in specific tissues. An example of this is a recent study in growth hormone releasing hormone knockout mice that examined circulating metabolites, and found mitochondrial metabolites were differentially regulated in circulation (Hoffman et al. 2020). Given the link between thermogenic adipose tissue activity and longevity (Darcy and Tseng 2019), metabolomic and lipidomic profiling of thermogenic adipose tissue from long-lived animals could provide new molecular targets to bridge the knowledge gap between these two physiological processes. Therefore, we performed metabolomic and lipidomic analyses on the BAT and inguinal white adipose tissue (iWAT) of Ames dwarf mice.

Here, we report a comprehensive dataset consisting of over 350 metabolites, 1100 structural lipids, and 100 oxylipins in BAT and iWAT of Ames dwarf mice. Structural lipid molecular species are presented in an interactive online viewer, allowing researchers to more easily analyze these data. Lipid changes we observed were consistent with increased thermogenic activity and insulin sensitivity, two key phenotypes of Ames dwarf mice. We also describe a unique pattern of oxylipin production between BAT and iWAT of Ames dwarf mice. Oxylipins are oxygenated products of polyunsaturated fatty acid (PUFA) metabolism, and are capable of acting as signaling molecules to regulate inflammation, glucose homeostasis, and lipid metabolism (Lynes et al. 2019). To demonstrate the validity and physiological relevance of our dataset, we demonstrate that not only is 5-hydroxyeicosapentaenoic acid (5-HEPE) increased in Ames dwarf BAT, but its abundance is correlated with BAT activity in other murine models of BAT activation or paucity. Moreover, 5-HEPE levels in human plasma are negatively correlated with important metabolic parameters, such as body mass index (BMI) homeostatic

model assessment-insulin resistance (HOMA-IR), and circulating triglyceride concentrations. Together, these data provide an in-depth look into the intersection of adipose tissue and aging, and offers a unique lipid signature for longevity.

Experimental model and subject details

Mice and treatments

All animal procedures were approved by the Institutional Animal Care and Use Committees at the Joslin Diabetes Center (JDC) and Southern Illinois University School of Medicine (SIUSOM). The animals were housed in conventional facilities under standard diurnal and temperature conditions (Atgl and Bmpr1a at JDC, and Ames dwarf at SIUSOM). Mice were fed standard chow diets (Purina 5020 at JDC, and Labdiet 5001 at SIUSOM). The age of the mice used were 6 months for male Ames dwarf mice, 10–18 weeks for male *Bmpr1a* knockout mice, and 7 weeks for male *Atgl* knockout mice. Ames dwarf mice are maintained in a closed breeding colony that avoids brother × sister mating on a heterogeneous background. Heterozygous sibling controls were used for Ames dwarf mice. For the *Atgl* and *Bmpr1a* knockout mice, floxed animals not expressing CRE were used as controls.

For experiments using acute cold exposure (*Atgl* knockout mice), mice were either maintained at room temperature of 23 °C or were placed at 4 °C for 1 h. For chronic cold exposure (*Bmpr1a* knockout mice), mice were housed at 30 °C or 4 °C for 48 h. For temperature manipulation, mice were individually housed with ad libitum access to food and water in temperature-controlled diurnal incubators (Caron Products & Services Inc.) that maintain their normal diurnal rhythm. At the time of sacrifice, serum was collected via cardiac puncture, mice were euthanized by cervical dislocation, and adipose tissue depots were collected. All tissues were snap frozen in liquid nitrogen and stored at − 80 °C until processing.

Study with humans of varying BMI

A cohort of 60 individuals were selected from the Leipzig Biobank (13 men and 47 women) to represent a wide variety of BMI. These individuals were categorized into lean (BMI < 25 kg/m^2), overweight (BMI 25.1–29.9 kg/

m^2), and obese (BMI > 30 kg/m^2). Metabolic data such as fasting glycemia, fasting insulin, HOMA-IR, and triglycerides were also quantified. All of the lean subjects had normal glucose tolerance (NGT). In the overweight group, there were 11 individuals with NGT, and 3 that were type 2 diabetic (T2D), while the obese group had 23 NGT individuals and 8 T2D individuals. The collection of the human samples, phenotyping, and serum analyses were approved by the ethics committee of the University of Leipzig (approval numbers: 159-12-21052012 and 017-12-23012012). All individuals provided written informed consent prior to entering the study.

Metabolomics

Frozen tissue samples were thawed at room temperature, then stored on ice. Thirty milligrams of tissue and a 0.4-ml extraction solvent mix were used for homogenization in 0.5-ml tubes. Volumes were adjusted accordingly for different tissue weights. Samples were homogenized with an Omni Bead Ruptor 24 having Cryo unit (Omni International, Kennesaw, GA, USA) for 2 min at 4 °C using ceramic beads. Tubes were centrifuged at 14,000*g* for 10 min at 4 °C. The clear supernatant was collected for further analysis. Metabolite extraction was achieved using a mixture of isopropanol:acetonitrile:water (3:3:2, by volume). Extracts were divided into three parts: 75 μl for gas chromatography combined with time-of-flight high-resolution mass spectrometry, 150 μl for reversed-phase liquid chromatography coupled with high-resolution mass spectrometry, and 150 μl for hydrophilic interaction chromatography with liquid chromatography and tandem mass-spectrometry. The NEXERA XR UPLC system (Shimadzu, Columbia, MD, USA) coupled with the Triple Quad 5500 System (AB Sciex, Framingham, MA, USA) was used to perform hydrophilic interaction liquid chromatography analysis, the NEXERA XR UPLC system (Shimadzu, Columbia, MD, USA) coupled with the Triple TOF 6500 System (AB Sciex, Framingham, MA, USA) to perform reversed-phase liquid chromatography analysis, and Agilent 7890B gas chromatograph (Agilent, Palo Alto, CA, USA) interfaced to a time-of-flight Pegasus HT mass spectrometer (Leco, St. Joseph, MI, USA). The GC system was fitted with a Gerstel temperature-programmed injector, cooled injection system (model CIS 4). An automated liner exchange (ALEX) (Gerstel, Muhlheim an der Ruhr, Germany) was used to eliminate cross-contamination from the sample matrix that was occurring between sample runs. Quality control was performed using a metabolite standards mixture and pooled samples. A standard quality control sample containing a mixture of amino and organic acids was injected daily to monitor mass spectrometer response. A pooled quality control sample was obtained by taking an aliquot of the same volume of all samples from the study and injected daily with a batch of analyzed samples to determine the optimal dilution of the batch samples and validate metabolite identification and peak integration. Collected raw data were manually inspected, merged, imputed, and normalized by the sample median.

Metabolomic data was analyzed as previously described (Tolstikov et al. 2014). Identified metabolites were subjected to pathway analysis with MetaboAnalyst 4.0, using metabolite set enrichment analysis (MSEA) module which consists of an enrichment analysis relying on measured levels of metabolites and pathway topology, and provides visualization of the identified metabolic pathways. Accession numbers of detected metabolites (HMDB, PubChem, and KEGG Identifiers) were generated, manually inspected, and utilized to map the canonical pathways. MSEA was used to interrogate functional relation, which describes the correlation between compound concentration profiles and clinical outcomes.

Structural lipidomics

Tissue samples were homogenized in 0.1× PBS with ceramic beads at 4 °C. 0.5-mg protein from homogenized tissue (determined by BCA) was used. Structural lipidomic analysis involved a modified Bligh and Dyer extraction utilizing a customized, automated liquid-liquid extraction sequence on a Hamilton Robotics StarLET Robot System. Four milliters of chloroform:MeOH (1:1, by volume) was added to the samples, followed by addition of a cocktail mixture of deuterium-labeled, odd chain, and extremely low naturally abundant internal standards. A front extraction was performed by adding 2 ml of 50 mM lithium chloride to sample tubes, vortexed in a multi tube vortexer for 3 min, and centrifuged at 1000*g* for 5 min, and the bottom chloroform layer was carefully transferred to a new glass tube. An additional 1.8 ml of chloroform was added to source tubes, vortexed, and centrifuged as described above, and transferred for a total of three chloroform transfers. The samples were dried down under a stream of nitrogen gas and resuspended in chloroform:MeOH (1:1, by

volume). A back extraction was performed for additional sample cleanup to remove contamination of protein, salts, and residual aqueous layer from front extraction. Two milliters of 10 mM lithium chloride was added to resuspended samples, and the same protocol was followed as the front extraction. Samples were dried, reconstituted in chloroform:MeOH (1:1, by volume), and stored at − 20 °C. Samples were prepared to run on the mass spectrometer by diluting 250× in isopropanol:methanol:acetonitrile:water (3:3:3:1, by volume) with 2 mM ammonium acetate.

Electrospray ionization (ESI) MS was performed on a Sciex TripleTOF 5600+ coupled with a direct injection loop on an Eksigent Ekspert MicroLC 200 system. The ESI DuoSpray Ion Source parameter settings were set to ion source gas 1 (GS1) at 10, ion source gas 2 (GS2) at 10, curtain gas (CUR) at 20, temperature at 300 °C, and ion spray voltage floating (ISVF) at 5500 V for positive mode and − 4500 V for negative mode. The MS/MS^{ALL} acquisition method consisted of two experiments, first a TOF MS survey scan acquiring data from 200 to 1200 m/z. The second experiment in the acquisition method consisted of 1000 high-resolution product ion scans with precursors evenly spaced from m/z 200.05 to m/z 1200.05 with 300 ms of accumulation time for each scan. The collision energy was set to 35 eV and − 35 eV for positive and negative modes, respectively, with a collision energy spread (CES) of ± 15 eV. Mass shift was controlled by a calibrant solution delivered every 10 samples at 500 μl/min by the atmospheric pressure chemical ionization (APCI) probe. The MS/MS^{ALL} data was acquired by Analyst TF 1.7 software (Sciex) and processed with MultiQuant 1.2.2.5 (Sciex) using an in-house database of lipid species for identification and quantification.

Signaling lipidomics

Tissue samples were homogenized in 0.1× PBS with ceramic beads at 4 °C. Depending on the analysis, either 100 μl of serum or 1 mg of protein from homogenized tissue (determined by BCA) was used. A mixture of deuterium-labeled internal standards was added to each aliquot, along with 3× volume of cold MeOH. Samples were vortexed for 5 min and stored overnight at − 20 °C. The following day,

the samples were centrifuged at 14,000g for 10 min, and the supernatant was added to a new tube containing 3 ml of acidified H_2O (pH 3.5) prior to the addition of C18 SPE. The methyl formate fractions were collected, dried under a nitrogen stream, and reconstituted in 50 μl of MeOH:H_2O (1:1 by volume). The samples were transferred to a fresh tube and centrifuged at 20,000g for 10 min at 4 °C. Thirty-five microliters of supernatant was transferred to LC-MS/MS vials for analysis using the BERG LC-MS/MS mediator lipidomics platform. The separation of the signaling lipids was done on an Ekspert MicroLC 200 system (Eksigent Technologies) with a Synergi™ Fusion-RP capillary C18 column (150 × 3 × 0.5 mm, 4 μm; Phenomenex Inc., Torrance, CA, USA) heated to 40 °C. A sample volume of 11 μl was injected at a flow rate of 20 μl/min. Lipids were separated using mobile phases A (100% H_2O, 0.1% acetic acid) and B (100% MeOH, 0.1% acetic acid) with a gradient starting at 60% B for 30 s, steadily increasing to 80% B by 5 min, reaching 95% B by 9 min, holding for 1 min, and then decreasing to 60% B by 12 min. MS analysis was performed on a SCIEX TripleTOF® 5600+ system using the HR-MRM strategy consisting of a TOF MS experiment looped with multiple MS/MS experiments. MS spectra were acquired in high-resolution mode (> 30,000) using a 100-ms accumulation time per spectrum. Full-scan MS/MS was acquired in high sensitivity mode, with an accumulation time optimized per cycle. Collision energy was set using rolling collision energy with a spread of 15 V. The identity of a component was confirmed using PeakView® software (SCIEX), and quantification was performed using MultiQuant™ software (SCIEX). C18 SPE cartridges were purchased from Biotage. All solvents were of HPLC or LC-MS/MS grade and were acquired from Sigma-Aldrich, Fisher Scientific, or VWR International.

Quantification and statistical analysis

No statistical method was used to predetermine sample size. The experiments were not randomized or blinded. All statistics were calculated using GraphPad Prism and Microsoft Excel. Between two groups, an unpaired Student's t test was done, and a two-way ANOVA followed by a Tukey's post hoc test was done for analysis of four groups. Correlations were generated based on Spearman

correlation tests. $P < 0.05$ was considered significant throughout the manuscript.

Results

Lipid metabolism is the major metabolic pathway altered in Ames dwarf adipose tissue

To assess alterations in metabolic pathways in the adipose tissue of long-lived animals in an unbiased manner, we performed metabolomic analysis in both BAT and iWAT of Ames dwarf and control mice. We identified 361 metabolites in both tissues. The normalized concentrations of all of the identified metabolites are included as supplements in Table S1. While we observed a distinct pattern of metabolite expression between Ames dwarf mice and controls in both BAT and iWAT (Supplemental Figs. 1a-1d), there was some overlap as well. For example, hydroxyisocaproic acid was among the top 10 altered metabolites in both BAT and iWAT, where it was very significantly increased in Ames dwarf mice (2.59-fold increase, $P = 0.0007$, in BAT and 2.40-fold increase, $P = 6.64E-6$ in iWAT, Fig. 1a, b). Hydroxyisocaproic acid is a metabolite of leucine metabolism. Indeed, MSEA revealed that valine, leucine, and isoleucine degradation had a strong trend to be increased in both BAT and iWAT of Ames dwarf mice (Fig. 1c, d). Elevated levels of branched-chain amino acids (BCAA) have been implicated in many aspects of metabolic syndrome, including diabetes, non-alcoholic fatty liver disease, and insulin resistance (Cheng et al. 2015; Iwasa et al. 2015; Newgard et al. 2009) Therefore, having fewer BCAA by way of degradation is consistent with the observed insulin sensitivity of Ames dwarf mice (Wiesenborn et al. 2014). Moreover, BCAA have been recently identified as fuel for thermogenically active BAT (Yoneshiro et al. 2019), which is consistent with the increased thermogenic activity seen in Ames dwarf mice. Other alterations that may be involved in longevity include arginine and aspartate metabolism, which were the two most upregulated pathways in iWAT. Indeed, arginine metabolism and aspartate metabolism were increased in Ames dwarf mice as many of the precursors in these pathways (e.g., arginine and asparagine) were decreased in Ames dwarf mice compared with controls, while the downstream products of these pathways (e.g., carbamoyl aspartate and urea) were increased in Ames dwarf mice (Fig. 1e). Interestingly, arginine metabolism is found to be highly upregulated in both BAT and iWAT following cold exposure (Lu et al. 2017), suggesting there is a metabolically

beneficial effect of increasing this pathway in Ames dwarf mice. While arginine metabolism was not increased in Ames dwarf BAT, aspartate metabolism, and the closely related urea cycle, trended to increase (data not shown).

Examining the MSEA of both BAT and iWAT, it was clear that pathways involved in lipid metabolism were consistently among the top altered metabolic pathways in both adipose depots (denoted in red in Fig. 1c, d). This is consistent with the notion that lipids constitute much of the mass of adipose tissue, that Ames dwarf mice lack several hormonal axes involved in lipid metabolism, and that Ames dwarf mice have a greatly reduced respiratory exchange ratio (RER) (Westbrook et al. 2009), suggesting that they utilize more lipids as metabolic fuel. To highlight the importance of lipid metabolism and thermogenesis, we plotted acylcarnitines (including free carnitine) identified in our metabolomics analysis which were significantly changed in BAT of Ames dwarf mice (carnitine synthesis by MSEA had a $P < 0.05$) (Fig. 1f). As can be seen, most of the acylcarnitines were increased in BAT of Ames dwarf mice. Acylcarnitines have been shown to be important fuel substrates for thermogenesis (Simcox et al. 2017). Moreover, we found that the acylcarnitines palmitoylcarnitine and myristoylcarnitine were increased in the BAT of Ames dwarf mice, and Simcox et al. demonstrated that these acylcarnitines were increased in plasma of mice exposed to cold, and that this increase was blunted in aged-mice. To further investigate the role of lipids in the metabolic function of adipose tissue in Ames dwarf mice, we performed a structural lipidomic analysis by using MS/MS^{ALL} shotgun lipidomics in both the BAT and iWAT. We only reported lipid molecular species if they were detectible in at least half of the samples of each adipose depot being analyzed. We were able to detect and quantify 1191 and 1083 structural lipids in BAT and iWAT, respectively (Supplemental Figs. 2a and 2b). The lipid
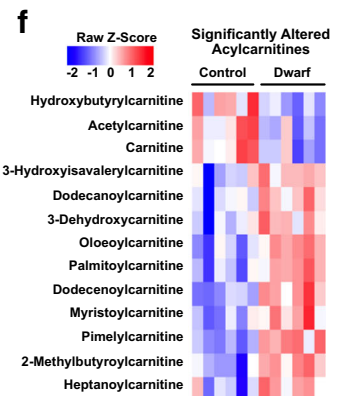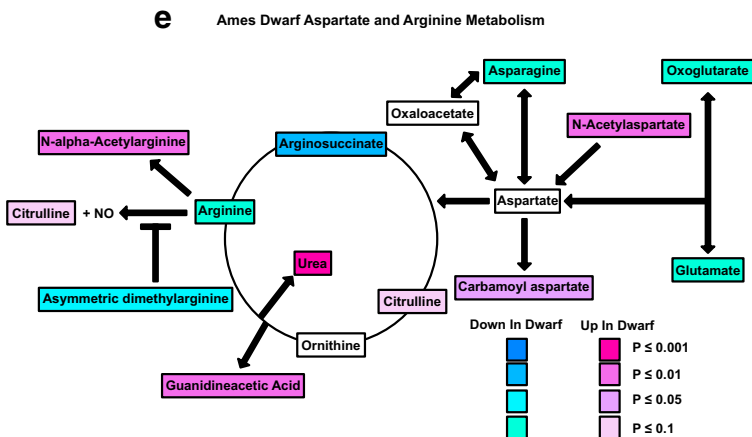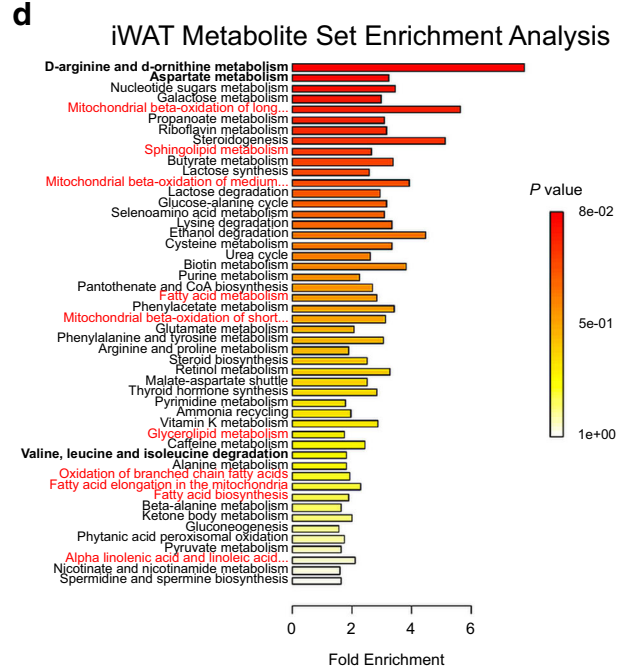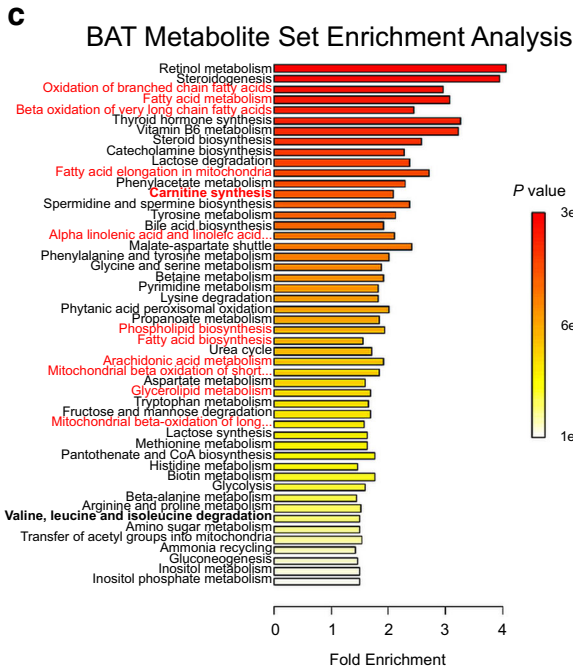
Fig. 1 Metabolomic analysis reveals Ames dwarf mice have altered ▶ lipid metabolism. **a** Top 10 altered metabolites in BAT of Ames dwarf mice. **b** Top 10 altered metabolites in iWAT of Ames dwarf mice. **c** Metabolite set enrichment analysis (MSEA) from BAT of Ames dwarf mice. The pathways involved in lipid metabolism are written in red. **d** MSEA from iWAT of Ames dwarf mice. **e** Schematic of differentially regulated metabolites in arginine and aspartate metabolism (by Student's t test). **f** Heatmap of significantly ($P < 0.05$ by Student's t test) regulated acylcarnitines in BAT from Ames dwarf mice. Each column represents one animal, and each row represents one acylcarnitine species. $N = 6$ per group in BAT, and $n = 6$ control and 9 dwarf in iWAT

a Top 10 Altered Metabolites in BAT

Metabolite	Fold Change	P Value
2-Hydroxybutyric Acid	3.26	1.26E-05
4-Pyridoxic Acid	5.04	2.26E-05
Pimelylcarnitine	3.01	0.0001
Dodecenoylcarnitine	2.95	0.0003
2-Furoylglycine	0.60	0.0005
Kynurenine	1.54	0.0006
Hydroxyisocaproic Acid	**2.59**	**0.0007**
N-Formylglycineamide Ribonucleotide	0.32	0.0008
Methionine	1.82	0.0008
Oleoylcarnitine	6.88	0.0010

b Top 10 Altered Metabolites in iWAT

Metabolite	Fold Change	P Value
Hydroxyisocaproic Acid	**2.40**	**6.64E-06**
Riboflavin	0.24	4.98E-05
Ribosylimidazole Acetic Acid	1.93	0.0002
3-Dehydroxycarnitine	1.80	0.0003
Dimethylsulfone	2.74	0.0004
Acetylcholine	1.85	0.0005
P-Cresol	5.16	0.0006
Urea	**2.58**	0.0006
4-Guanidinobutanoic Acid	2.65	0.0007
Fapy-Adenine	0.57	0.0008

c BAT Metabolite Set Enrichment Analysis

d iWAT Metabolite Set Enrichment Analysis

e Ames Dwarf Aspartate and Arginine Metabolism

f Significantly Altered Acylcarnitines

classes identified were acylcarnitine (AC), ceramide (Cer), cholesterol ester (CE), coenzyme Q (CoQ), monoacylglycerol (MAG), diacylglycerol (DAG), triacylglycerol (TAG), free fatty acid (FFA), glycolipid, phosphatidic acid (PA), phosphatidylcholine (PC), phosphatidylethanolamine (PE), phosphatidylglycerol (PG), phosphatidylinositol (PI), phosphatidylserine (PS), sphingomyelin (SM), cardiolipin (CL), and branched fatty acid esters of hydroxy fatty acids (FAHFA). The data from each of these lipid species are presented in the supplemental data as Tables S2 and S3.

To assess which lipid classes were the most altered in Ames dwarf mice, we normalized the lipids changed to the total detected per each family to calculate the percent of each lipid family that was significantly altered. Interestingly, we observed that in BAT, Ames dwarf mice had an increase in FAHFA, and FFA, and a decrease in ceramides (Fig. 2a), while iWAT in Ames dwarf mice had a downregulation of many lipid classes, including phospholipids, FAHFA, and ceramides (Fig. 2b). To further identify lipid species that were significantly altered in Ames dwarf adipose tissue, we plotted significantly altered lipid species ($P < 0.05$) on heatmaps. We identified 110 significantly altered lipids in BAT and 244 significantly altered lipids in iWAT (Fig. 2c, d). Analysis of the heatmaps illustrated distinct changes, which were further elaborated below. These alterations were also clearly demonstrated on volcano plots (Supplemental Figs. 2c and 2d). To ease the analysis of these datasets by other researchers, we created an interactive online viewer that can be found at https://jdreyf.shinyapps.io/darcy_ames_adipose/ (Fig. 2e). This interactive viewer plots the structural lipidomic data by tissue depot (depicted by shape) and by lipid class (depicted by color). The size of the shape is proportional to its P value, such that larger symbols represent increased significance. The plot is graphed as the abundance of lipids in dwarfs (Y-axis) vs the abundance of lipids in controls (X-axis). The scales of the X-and Y-axes are on a log10 scale so that all points above the $X = Y$ line are increased in dwarf adipose tissue, and all points below the $X = Y$ line are increased in control adipose tissue. For example, when examining cardiolipin species in BAT and iWAT, we can see most of the points are above the $Y = X$ line, indicating there is an overall trend for Ames dwarf mice to possess increased cardiolipin (Fig. 2f).

Lipid changes in Ames dwarf adipose tissue are associated with increased thermogenesis and insulin sensitivity

Cardiolipin is an integral lipid in the inner mitochondrial membrane (Joshi et al. 2009). Recent reports have demonstrated that remodeling of low-abundant cardiolipin species is particularly important to thermogenic function (Lynes et al. 2018; Sustarsic et al. 2018). While the overall abundance of cardiolipin tended to increase in both BAT and iWAT when comparing dwarf vs control, it did not reach statistical significance ($P = 0.11$ and $P = 0.59$ for BAT and iWAT, respectively). We did, however, observe an increase in 5% of cardiolipin species in BAT and 9% of cardiolipin species in iWAT. The significantly altered cardiolipin species are depicted in Figs. 3 a and b, and Supplemental Figs. 2c and 2d. Critically, this is in keeping with the reported increased thermogenic activity of Ames dwarf mice. Another important phenotype of Ames dwarf mice is their extreme insulin sensitivity. Therefore, it was conceivable that levels of ceramides, which are well known to cause insulin resistance (Chavez and Summers 2012; Ussher et al. 2010), were decreased in the adipose tissue of Ames dwarf mice (Fig. 3c, d and Supplemental Figs. 2c and 2d). Not only were individual species of ceramides altered, but the total concentration of ceramides in each depot were also drastically decreased

Fig. 2 Ames dwarf mice have an altered adipose structural lipidome. **a** The percentage of lipids in each class that were significantly ($P < 0.05$ by Student's t test) increased or decreased in BAT of Ames dwarf mice. The lipid classes are acylcarnitine (AC), ceramide (Cer), cholesterol ester (CE), coenzyme Q (CoQ), monoacylglycerol (MAG), diacylglycerol (DAG), triacylglycerol (TAG), free fatty acid (FFA), glycolipid, phosphatidic acid (PA), phosphatidylcholine (PC), phosphatidylethanolamine (PE), phosphatidylglycerol (PG), phosphatidylinositol (PI), phosphatidylserine (PS), sphingomyelin (SM), cardiolipin (CL), and branched fatty acid esters of hydroxy fatty acids (FAHFA). **b** The percentage of lipids in each class that were significantly increased or decreased in iWAT of Ames dwarf mice. **c** Heatmap showing the relative lipid concentration of individual lipid species that were significantly (P value < 0.05 by Student's t test) different between Ames dwarf mice and controls in BAT. Each column represents one animal, and each row represents one lipid species ($n = 6$ control and 5 dwarf). **d** Heatmap showing the relative lipid concentration of individual lipid species that were significantly different between Ames dwarf mice and controls in iWAT ($n = 6$ control and 9 dwarf). **e** Representation from an online viewer of structural lipids in dwarf vs control adipose tissue. **f** Representation from the online viewer examining cardiolipin in BAT and iWAT
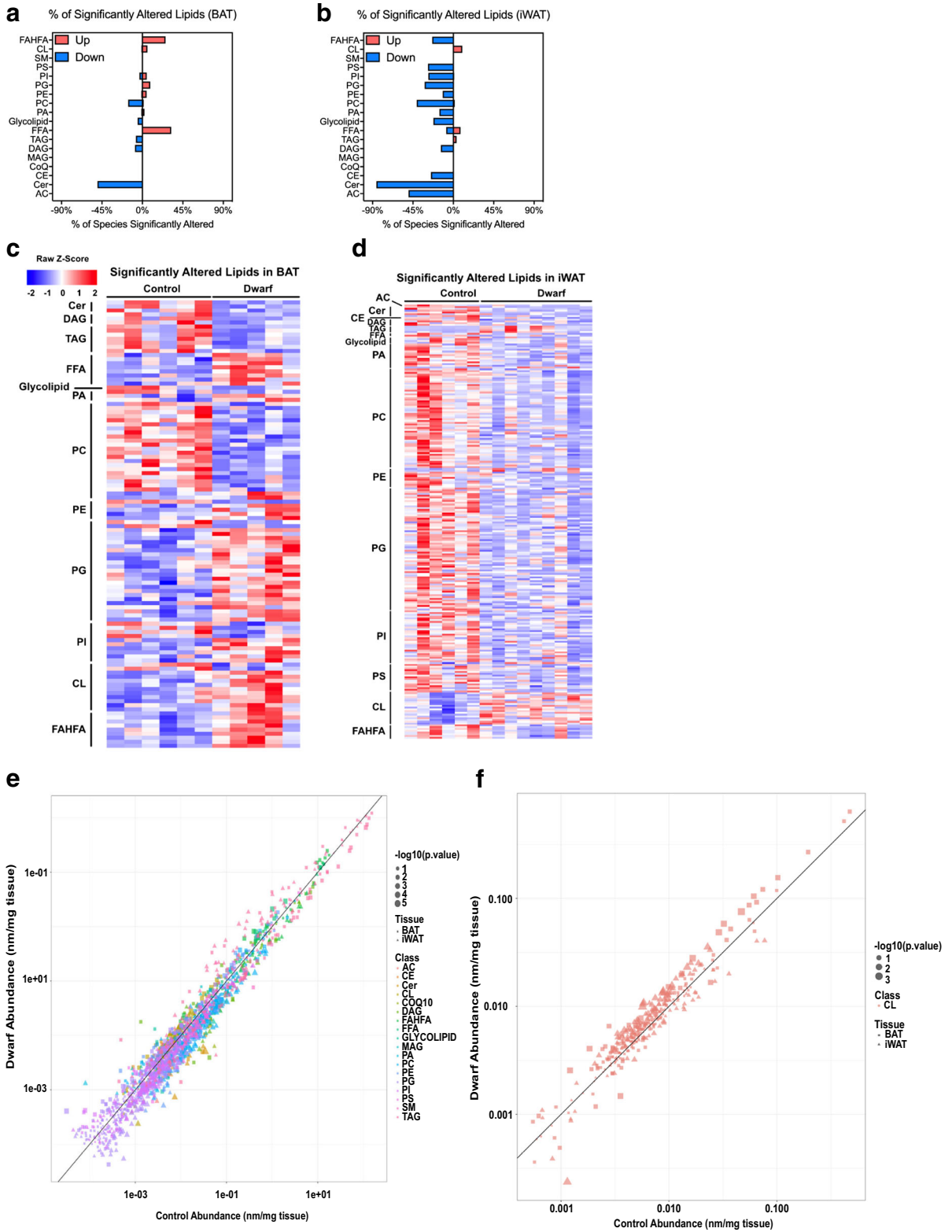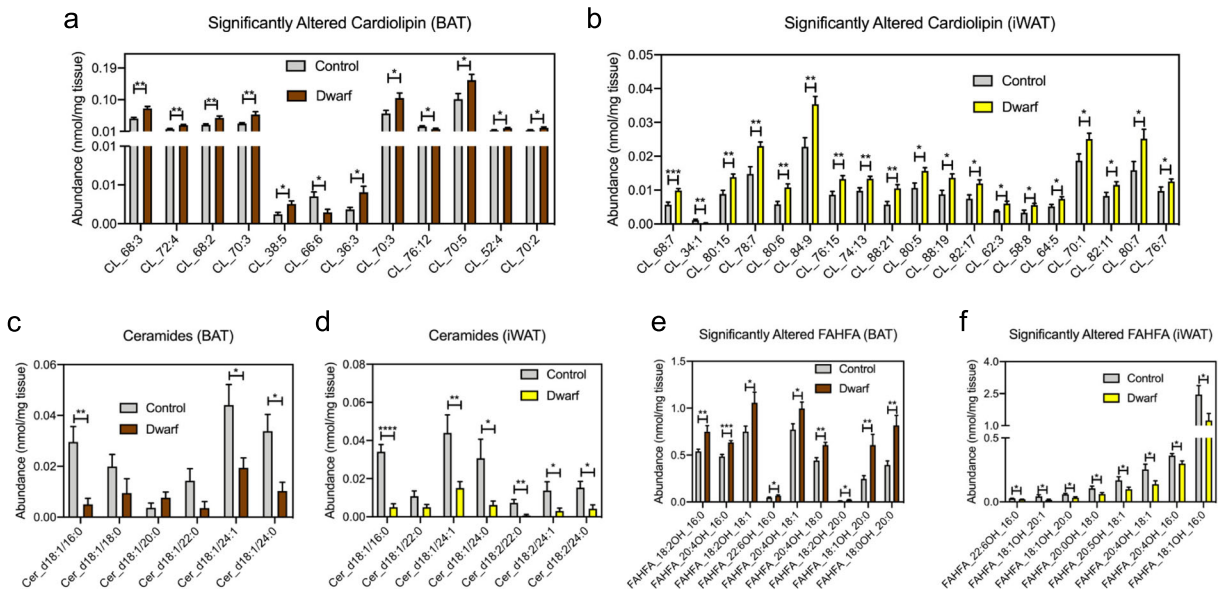
Fig. 3 Ames dwarf mice have altered lipids involved in thermogenesis and insulin sensitivity. **a** Concentrations of significantly altered cardiolipin in BAT from Ames dwarf mice. **b** Concentrations of significantly altered cardiolipin in iWAT from Ames dwarf mice. **c** Concentrations of all quantified ceramides in BAT of Ames dwarf mice. **d** Concentrations of all quantified ceramides in iWAT of Ames dwarf mice. **e** Concentrations of significantly altered branched fatty acid esters of hydroxy fatty acids (FAHFA) in BAT from Ames dwarf mice. **f** Concentrations of significantly altered FAHFA in iWAT from Ames dwarf mice. Data throughout the figure are presented as mean ± SEM; $n = 6$ control and 5 dwarf for BAT; $n = 6$ control and 9 dwarf for iWAT. *$P < 0.05$, **$P < 0.01$, ***$P < 0.001$, ****$P < 0.0001$ by Student's t test

($P = 0.0001$ and $P = 7.06E{-}07$ for BAT and iWAT, respectively). Some lipid classes that are believed to be beneficial had opposite regulation between iWAT and BAT in Ames dwarf mice. FAHFA are a fairly new lipid class that exerts anti-diabetic and anti-inflammatory effects (Yang et al. 2018; Yore et al. 2014). Their biosynthesis is stimulated by increased uptake of glucose into adipocytes by the transcription factor carbohydrate-responsive element-binding protein (Yore et al. 2014), although their biosynthetic pathway is not fully understood. The total concentration of FAHFA tended to increase in Ames dwarf BAT ($P = 0.11$), while the total concentration of FAHFA decreased by nearly 50% in iWAT ($P = 0.06$). Interestingly, while total concentrations of FAHFA in BAT and iWAT were not significantly altered between control and dwarf mice, the abundance of several individual FAHFA species was significantly increased in BAT and decreased in iWAT of Ames dwarf mice (Fig. 3e, f and Supplemental Figs. 2c and 2d).

A major change we observed in iWAT between Ames dwarf mice and controls was in phospholipids, although we observed no alterations in phospholipid composition between dwarfs and controls in BAT (Supplemental Figs.

3a–3h). In iWAT, the total concentration of phospholipid classes was significantly decreased in nearly every class of phospholipids (Fig. 4a); however, this was not true of lyso-containing phospholipids (Fig. 4b). A more in-depth analysis demonstrated that while saturated phospholipid concentrations were decreased in Ames dwarf mice, the differences between dwarf and control mice were more significant in monounsaturated phospholipids, and larger still in polyunsaturated phospholipids (Fig. 4c–e). The decrease in polyunsaturated lipids we observed has also been reported in other long-lived models and is believed to confer longevity since polyunsaturated lipids are more prone to oxidative damage (Hulbert et al. 2006a; Hulbert et al. 2006b). In agreement with this, Ames dwarf mice have been reported to have lower levels of reactive oxygen species (ROS) (Rojanathammanee et al. 2014; Sharma et al. 2010). Linoleic acid (18:2), arachidonic acid (20:4), and docosahexaenoic acid (22:6) are critical ω-3 and ω-6 long-chain PUFAs that can be stored in phospholipids. In iWAT, the phospholipids that contain the molecular species 18:2, 20:4, and 22:6 were all decreased in Ames dwarf mice (Fig. 4f–h). Intriguingly, exercise has also been shown to improve insulin sensitivity in iWAT (Stanford et al. 2015) and decrease iWAT
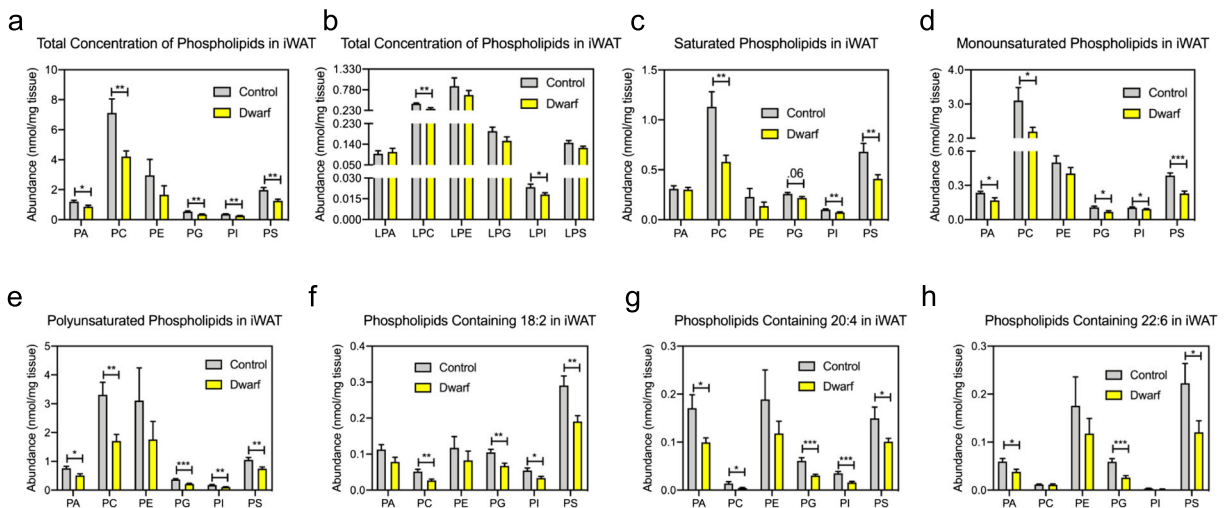
Fig. 4 Ames dwarf mice have decreased phospholipids in their iWAT. **a** Concentrations of phospholipids in iWAT of Ames dwarf mice. **b** Concentrations of lyso-containing phospholipids in iWAT of Ames dwarf mice. **c** Concentrations of saturated phospholipids in iWAT of Ames dwarf mice. **d** Concentrations of monounsaturated phospholipids in iWAT of Ames dwarf mice. **e** Concentrations of polyunsaturated phospholipids in iWAT of

Ames dwarf mice. **f** Concentrations of phospholipids containing 18:2 in iWAT of Ames dwarf mice. **g** Concentrations of phospholipids containing 20:4 in iWAT of Ames dwarf mice. **h** Concentrations of phospholipids containing 22:6 in iWAT of Ames dwarf mice. Data throughout the figure are presented as mean ± SEM; $n = 6$ control and 9 dwarf. $*P < 0.05$, $**P < 0.01$, $***P < 0.001$ by Student's t test
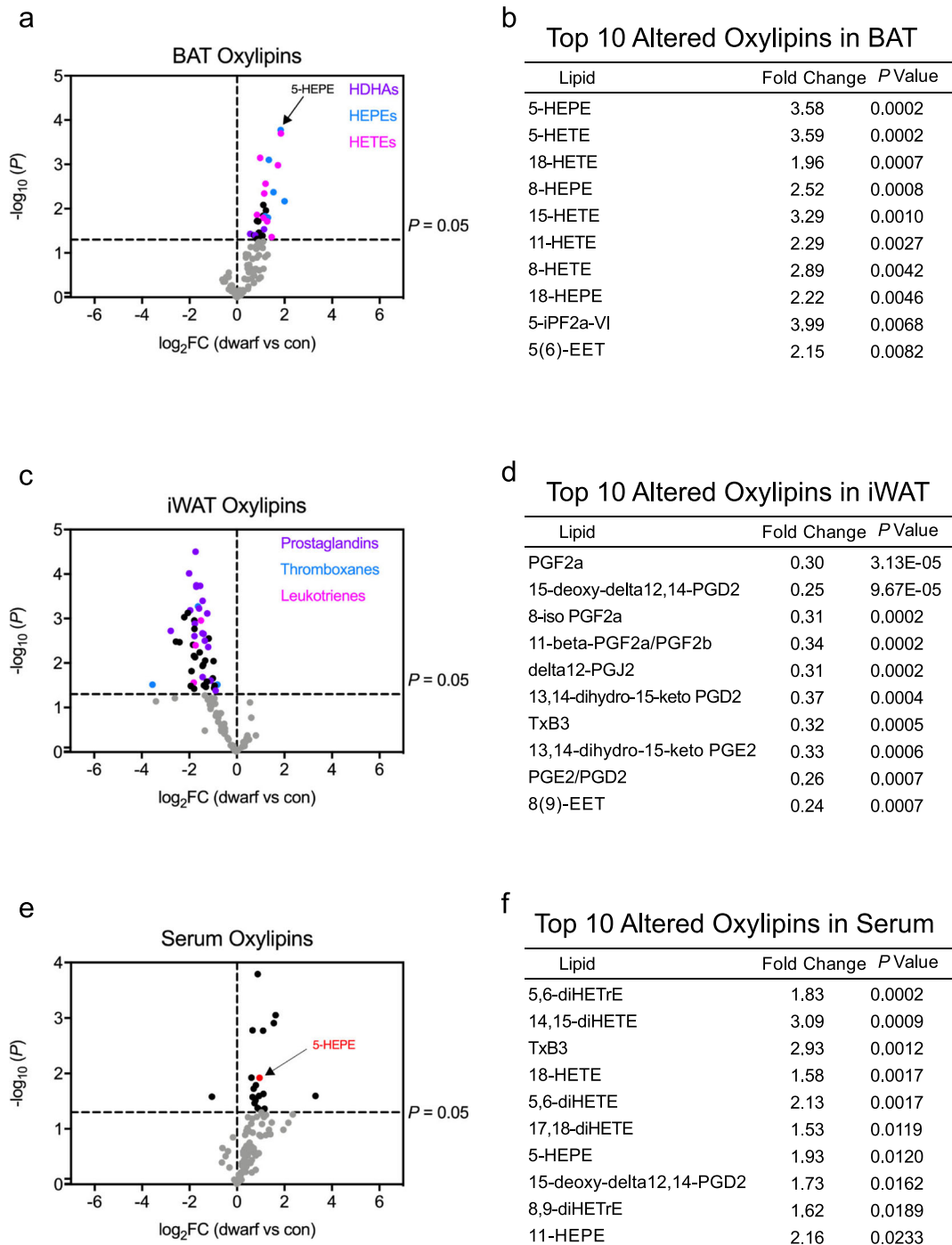
phospholipid content (May et al. 2017), suggesting that decreased iWAT phospholipid content may aid in the insulin sensitivity of Ames dwarf mice. While the role of phospholipids in insulin sensitivity in adipose tissue has yet to be established, decreased phospholipid content in muscle has been shown to improve insulin sensitivity (Andersson et al. 1998; Goto-Inoue et al. 2013).

5-HEPE is increased in models of BAT activation and is negatively correlated with critical metabolic parameters in humans

While lipids are integral parts of cell and organelle membranes, their roles as signaling molecules have garnered greater attention in recent years. We have recently identified two oxylipins that are produced by activated BAT. 12,13-Dihydroxy-9Z-octadecenoic acid (12,13-diHOME) is secreted from BAT and acts in an autocrine/paracrine manner to stimulate lipid uptake, and 12-hydroxyeicosapentaenoic acid (12-HEPE) works in an endocrine manner to promote glucose homeostasis (Leiria et al. 2019). Importantly, the concentrations of both 12,13-diHOME and 12-HEPE are increased in BAT and serum following BAT activation through sympathetic nervous system activation (e.g., cold exposure). Since no biosignature of oxylipins exists in long-lived mice, we examined if oxylipins were

differentially regulated in Ames dwarf mice. The oxylipin data from BAT, iWAT, and serum are presented in Table S4. We observed an upregulation of hydroxydocosahexaenoic acid (HDHA), HEPE, and hydroxyeicosatetraenoic acid (HETE) lipids in BAT of Ames dwarf mice (Fig. 5a, b). Importantly, the downstream byproducts of HDHA and HEPE lipids have been shown to have anti-inflammatory properties (Spite et al. 2014). In iWAT, we noticed that the dwarf mice displayed a distinct decrease of well-known proinflammatory lipid mediators, namely prostaglandins, thromboxanes, and leukotrienes (Fig. 5c, d). The alterations in pro- and anti-inflammatory lipid mediators described here are consistent with the reported inflammatory profile of Ames dwarf mice (Masternak and Bartke 2012), as well as their extended metabolic healthspan and lifespan.

To determine which of these signaling lipids could be secreted from the BAT of Ames dwarf mice, we also assessed oxylipin concentrations in serum of Ames dwarf mice (Fig. 5e, f). One of the most highly upregulated oxylipins in serum from Ames dwarf mice was (14R,15S)-14,15-dihydroxy-5Z,8Z,10E,12E-icosatetraenoic acid (14,15-diHETE). Interestingly, 14,15-diHETE has been shown to have anti-inflammatory properties by inhibiting natural killer cells (Ramstedt et al. 1984). Indeed, 14,15-diHETE was also increased in Ames dwarf BAT by a 2.15-fold increase ($P =$

a

BAT Oxylipins

b

Top 10 Altered Oxylipins in BAT

Lipid	Fold Change	P Value
5-HEPE	3.58	0.0002
5-HETE	3.59	0.0002
18-HETE	1.96	0.0007
8-HEPE	2.52	0.0008
15-HETE	3.29	0.0010
11-HETE	2.29	0.0027
8-HETE	2.89	0.0042
18-HEPE	2.22	0.0046
5-iPF2a-VI	3.99	0.0068
5(6)-EET	2.15	0.0082

c

iWAT Oxylipins

d

Top 10 Altered Oxylipins in iWAT

Lipid	Fold Change	P Value
PGF2a	0.30	3.13E-05
15-deoxy-delta12,14-PGD2	0.25	9.67E-05
8-iso PGF2a	0.31	0.0002
11-beta-PGF2a/PGF2b	0.34	0.0002
delta12-PGJ2	0.31	0.0002
13,14-dihydro-15-keto PGD2	0.37	0.0004
TxB3	0.32	0.0005
13,14-dihydro-15-keto PGE2	0.33	0.0006
PGE2/PGD2	0.26	0.0007
8(9)-EET	0.24	0.0007

e

Serum Oxylipins

f

Top 10 Altered Oxylipins in Serum

Lipid	Fold Change	P Value
5,6-diHETrE	1.83	0.0002
14,15-diHETE	3.09	0.0009
TxB3	2.93	0.0012
18-HETE	1.58	0.0017
5,6-diHETE	2.13	0.0017
17,18-diHETE	1.53	0.0119
5-HEPE	1.93	0.0120
15-deoxy-delta12,14-PGD2	1.73	0.0162
8,9-diHETrE	1.62	0.0189
11-HEPE	2.16	0.0233

Fig. 5 Ames dwarf mice have an altered oxylipin profile. **a** Volcano plot of oxylipins from BAT in dwarfs vs controls displayed as the log base-2 ratio of dwarf to control versus the inverse log base-10 of the P value of this comparison (Student's t test). A P value of 0.05 is indicated by a dotted line. Hydroxydocosahexaenoic acid (HDHA), hydroxyeicosapentaenoic acid (HEPE), and hydroxyeicosatetraenoic acid (HETE) family members are denoted ($n = 6$ per group). **b** Top 10 altered oxylipins in BAT. **c** Volcano plot of oxylipins from iWAT ($n = 6$ control and 9 dwarf). **d** Top 10 altered oxylipins in iWAT. **e** Volcano plot of oxylipins from serum ($n = 9$ per group). **f** Top 10 altered oxylipins in serum

0.01) (Supplemental Table 4). Importantly, we found that the most significantly upregulated oxylipin in BAT, 5-HEPE, was also increased in Ames dwarf serum (Fig. 6a). 5-HEPE is a metabolite of 5-lipoxygenase activity from eicosapentaenoic acid (EPA), an ω-3 PUFA. To determine whether 5-HEPE was produced by activated BsAT, we measured 5-HEPE content in the BAT of a mouse model with severe BAT paucity ($Myf5^{Cre}BMPr1a^{fl/fl}$ mice), which possess impaired bone morphogenic protein (BMP) signaling in brown adipocyte precursors (Schulz et al. 2013). The control mice had a notable increase of 5-HEPE in their BAT following 48 h of cold exposure (Fig. 6b). However, the induction of 5-HEPE in response to cold was significantly diminished in the $Myf5^{Cre}BMPr1a^{fl/fl}$ mice, suggesting that active BAT is necessary for its production. We had previously shown that liberating oxylipins and/or their precursors from triglycerides is a critical step in their secretion (Leiria et al. 2019). Indeed, while 1 h of cold exposure was sufficient to raise 5-HEPE levels in the serum of control animals, deletion of adipose triglyceride lipase (ATGL) in adipose tissue greatly reduced the circulating level of 5-HEPE in response to cold (Fig. 6c). For translatability, we examined 5-HEPE concentrations in plasma of a cohort of human subjects with a wide range of BMI. We found that lean patients (BMI < 25 kg/m^2) had significantly more 5-HEPE than overweight and obese patients (BMI > 25 kg/m^2) (Fig. 6d). Indeed, plasma levels of 5-HEPE were negatively correlated with critical metabolic parameters such as BMI, HOMA-IR, circulating triglyceride concentrations, and alanine transaminase (ALAT) (Fig. 6e–h). It is worth noting that these subjects were not age-matched, although 5-HEPE did not correlate with age. Taken together, these data suggest that 5-HEPE is secreted by activated BAT and may contribute to the improved metabolism, extended healthspan, and delayed aging phenotypes of Ames dwarf mice.

Discussion

Lipid metabolism is the major metabolic pathway altered in Ames dwarf adipose tissue

Ames dwarf mice are exceptionally long-lived and have an improved metabolic healthspan. Growing evidence suggests that adipose tissue plays a key role in the metabolic healthspan of long-lived animals with GH-related mutations (Darcy et al. 2017). For example, adipose tissue from Ames dwarf mice, and the similar Snell dwarf mouse, has been shown to have delayed preadipocyte senescence,

increased glucose disposal, increased thermogenic activity, increased adiponectin secretion, and decreased pro-inflammatory secretion (e.g., TNF-α), among other favorable phenotypes (Darcy et al. 2016; Masternak and Bartke 2012; Stout et al. 2014; Wiesenborn et al. 2014). Despite this knowledge, the underlying metabolic pathways that control these phenotypes have remained poorly understood. Here, we provide evidence that lipid metabolism may underlie the beneficial phenotypes observed in the adipose tissue of Ames dwarf mice, including increased concentrations of cardiolipin, decreased concentrations of ceramides, and a decrease in pro-inflammatory oxylipins in iWAT. Moreover, we demonstrate that 5-HEPE is increased during BAT activation, and that it is negatively correlated with critical metabolic phenotypes. These findings are summarized in Fig. 6 i.

To identify which metabolic pathways may underlie the altered phenotypes seen in adipose tissue of long-lived mice, we performed a metabolomic analysis of the iWAT and BAT of Ames dwarf mice. Interestingly, we found that the closely related arginine metabolism and aspartate metabolism were upregulated in iWAT. Indeed, it has been shown that both amino acids play a role in the aging process. For example, arginine supplementation has been shown to reverse the age-related decline in renal function (Reckelhoff et al. 1997). Moreover, nitric oxide (NO), a product of arginine metabolism, is beneficial to an aging cardiovascular system (Sverdlov et al. 2014). Indeed, our model suggests there may be an increase in NO in Ames dwarf mice, which supports the observation of decreased cardiac collagen in those mice (Helms et al. 2010). Aspartate supplementation reduces ROS production in neuroblastoma cells (Delic et al. 2017) and increases antioxidant levels in the blood of pigs (Duan et al. 2016; Ni et al. 2016). Moreover, aspartate supplementation was able to reduce oxidative stress in rat testes (Oh et al. 2002). Indeed, decreased ROS is believed to be a major mechanism behind the extended lifespan and healthspan of Ames dwarf mice (Brown-Borg and Rakoczy 2003; Rojanathammanee et al. 2014; Romanick et al. 2004; Sharma et al. 2010). Furthermore, aspartate metabolism was recently shown to be highly altered in sera from calorie-restricted non-human primates (Aon et al. 2020). Our findings highlight a clear role for arginine and aspartate metabolism in metabolic healthspan. Beyond arginine and aspartate metabolism, we did observe metabolite alterations in Ames dwarf adipose tissue that have been previously reported to be associated with

longevity. For example, calorie restriction in mice has been shown to increase catecholamine production in BAT (Green et al. 2020). MSEA in BAT of Ames dwarf mice also revealed increased catecholamine biosynthesis (Fig. 1c).

Lipid changes in Ames dwarf adipose tissue are associated with increased thermogenesis and insulin sensitivity

Lipid metabolism is clearly the most differentially regulated metabolic pathway in Ames dwarf adipose tissue. Highlighting this, we demonstrate that Ames dwarf mice have an increase in the abundance of acylcarnitines, which have been shown to be a metabolic substrate for thermogenesis (Simcox et al. 2017). Interestingly, carnitine treatment in old mice stimulates acylcarnitine production and protects against age-related cold sensitivity, suggesting that acylcarnitine availability may play a role in the age-related decline in BAT function. Indeed, there is a downregulation in serum carnitines in humans with frailty (Rattray et al. 2019), although a relationship between carnitines, frailty, and BAT has not yet been established in humans. To further understand how lipid metabolism is altered, we use a structural lipidomic analysis and identify that Ames dwarf mice exhibit alterations in molecular lipid species that are consistent with their increased insulin sensitivity and thermogenic activity. For example, Ames dwarf mice have an increase in the abundance of specific cardiolipin molecular species, a reduction in the abundance of ceramides, and a decrease in the abundance of iWAT phospholipids. Interestingly, cardiolipin has been reported to decrease with age in the brain and heart of rats (Paradies et al. 2010), and ceramides have been shown to increase with age in *Caenorhabditis elegans* and humans (Cutler et al. 2014; Huang et al. 2014). This is therefore in keeping with our finding that specific cardiolipin molecular species are increased, and ceramides are decreased, in long-lived Ames dwarf mice. Importantly, ceramide-rich diets shorten lifespan in *C. elegans* (Cutler et al. 2014). Additionally, caloric restriction, possibly the best-known intervention to extend longevity, decreases ceramide levels (Green et al. 2017). Moreover, decreased ceramides are associated with increased beiging in subcutaneous adipose tissue (Chaurasia et al. 2016). Our ceramide data from Ames dwarf mice adds to the body of literature that suggests ceramides play a crucial role in the aging process. Our finding that Ames dwarf mice have a decrease in polyunsaturated phospholipids is somewhat contradictory to a previously reported study that states Ames dwarf mice do not have decreased polyunsaturated

phospholipids (Valencak and Ruf 2013); however, this study did not include adipose tissue and primarily focused on membrane lipids, indicating that the changes in lipid profiles in this long-lived animal model could be tissue-specific. While many lipid classes have similar alterations in the iWAT and BAT between Ames dwarfs and controls, FAHFA has complete opposite regulation. The increase in FAHFA levels in BAT with the concurrent decrease in the levels of FAHFA in iWAT highlights the possibility of previously unknown regulation of FAHFA biosynthesis and/or catabolism that is depot-dependent, and is potentially associated with lifespan and/or healthspan. Further explorations are warranted. Along with alterations in structural lipids, we observe distinct regulation of oxylipins between iWAT and BAT. In BAT, there is a clear upregulation of HEPEs, HDHAs, and HETEs. Although HETEs can be pro-inflammatory, HEPEs and HDHAs can act as anti-inflammatory mediators, by giving rise to specialized pro-resolving molecules (Serhan and Levy 2018). The anti-inflammatory effects of these molecules are hypothesized to be at least partially responsible for the anti-inflammatory effects of ω-3 PUFAs. In iWAT, there is a clear decrease in pro-inflammatory prostaglandins, thromboxanes, and leukotrienes. Indeed, this shift from pro- to anti-inflammatory lipids is consistent with the published literature surrounding Ames dwarf mice and is consistent with what is expected from a long-lived animal since chronic, sterile inflammation is believed to accelerate the aging process (Masternak and Bartke 2012). Indeed, treating *C. elegans* and mice with aspirin, which inhibits cyclooxygenase activity (and therefore the production of prostaglandins and thromboxanes), extends longevity (Ayyadevara et al. 2013; Strong et al. 2008). Intriguingly, it seems the effects of aspirin on aging recapitulate the effects of calorie restriction in mice and

Fig. 6 5-HEPE is increased in BAT activation. **a** 5-Hydroxyeicosapentaenoic acid (HEPE) concentrations in BAT and serum of Ames dwarf and control mice. $n = 6$ in BAT and $n = 9$ in serum. ******$P < 0.01$ by Student's t test. **b** 5-HEPE concentrations in BAT from *Bmpr1a* KO mice and controls housed at 30 °C or 4 °C for 48 h. $n = 5$, except 30 °C KO where $n = 4$. *****$P < 0.05$ by Student's t test. **c** 5-HEPE concentrations in serum from *Atgl* KO mice and controls housed at 23 °C or 4 °C for 1 h. $n = 5$, except controls housed at 23 °C where $n = 4$. *****$P < 0.05$ by two-way ANOVA with a Tukey post hoc analysis. **d** 5-HEPE concentrations in humans that are lean (BMI < 25 kg/m^2), overweight (BMI = 25.1–29.9 kg/m^2), and obese (BMI > 30 kg/m^2). $n = 14$–31, ********$P < .0001$ by one-way ANOVA with a Tukey post hoc analysis. **e–h** Spearman's correlation between the plasma level of 5-HEPE and BMI, HOMA-IR, circulating triglycerides, and ALAT from human subjects ($n = 60$). **i** Graphical summary of findings from the present study. The red start indicates novel molecular characteristics defined in our study
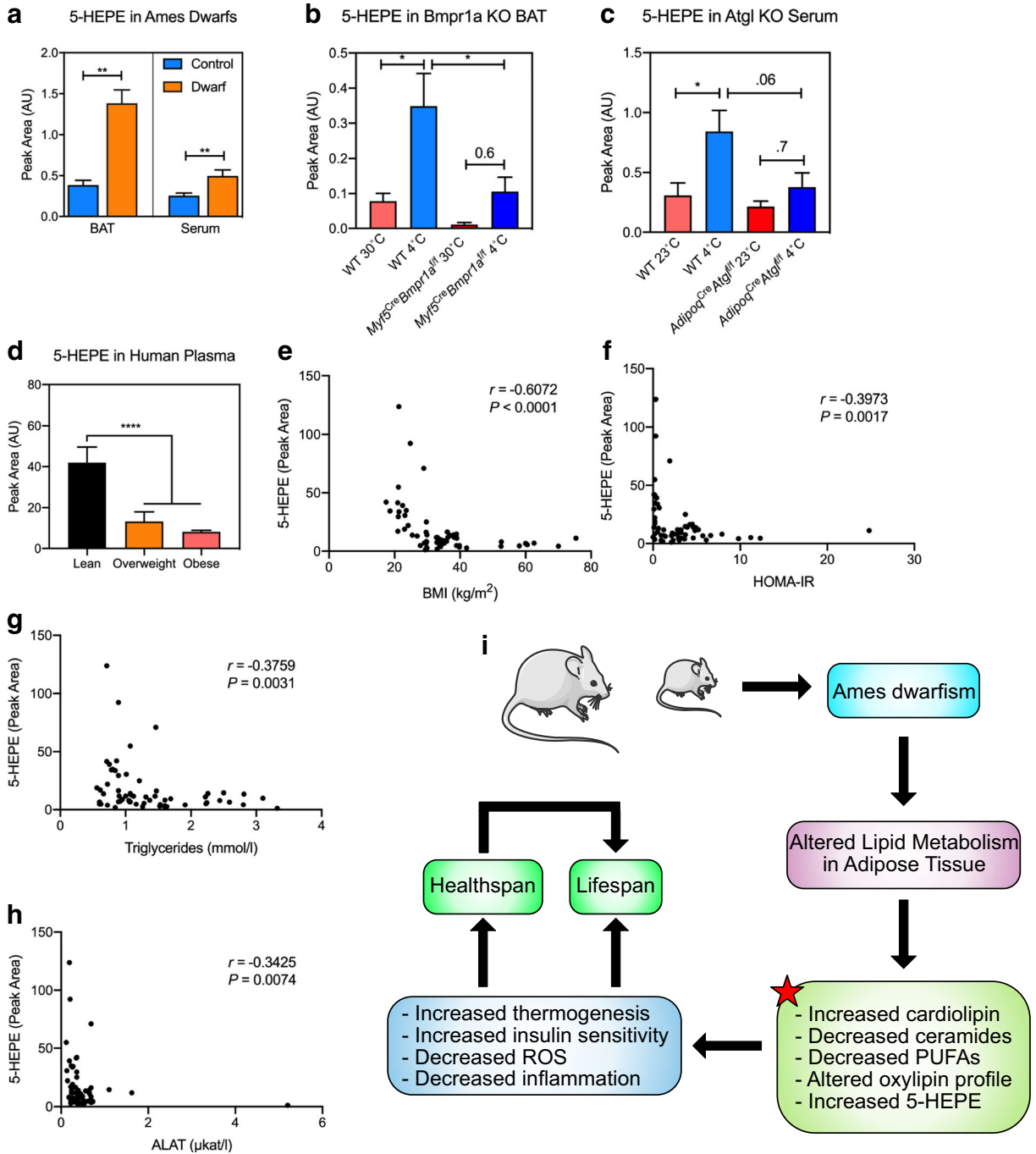
worms (Pietrocola et al. 2018), and act through the activation of DAF-16 in worms (Wan et al. 2013). To what extent prostaglandins and thromboxanes contribute to the aging process of these systems has not yet been elucidated.

5-HEPE is increased in models of BAT activation and is negatively correlated with critical metabolic parameters in humans

Adding to the validity and physiological relevance of our dataset, we identify a novel lipid batokine, 5-HEPE. 5-HEPE is not only the most significantly upregulated oxylipin in BAT of Ames dwarf mice but is also increased in their serum. Although there is limited prior research on 5-HEPE, it is believed to act through G protein–coupled receptor (GPCR) 119 and 120. Indeed, through GPCR 119/120 action, 5-HEPE has been shown to induce regulatory T cells (Tregs) and induce the secretion of insulin and glucagon-like peptide-1 (GLP-1) (Kogure et al. 2011; Onodera et al. 2017). Moreover, 5-HEPE has been shown to decrease adipose tissue inflammation in the context of high-fat diet in mice as well as activate nuclear factor erythroid 2–related factor 2 (Nrf2), a regulator of oxidative stress (Nagahora et al. 2017; Wang et al. 2017). Interestingly, Nrf2 activation through Protandim was shown to increase longevity (Strong et al. 2016). Here, we use BAT activation through cold exposure, and BAT paucity through the deletion of the Bmpr1a gene, to show that 5-HEPE is produced from activated BAT. Indeed, the induction of 5-HEPE in BAT following cold exposure is absent in mice with severe BAT paucity. As with other BAT-derived lipokines that our laboratory has discovered (Leiria et al. 2019), ATGL-mediated lipolysis is necessary to increase 5-HEPE abundance in circulation following cold exposure. The specific mechanism for how ATGL mediates the production of these lipokines warrants further investigation. For translatability, we looked to determine 5-HEPE abundance in circulation from human subjects with a wide range of BMI. Importantly, we find that 5-HEPE is significantly and negatively correlated with BMI, HOMA-IR, circulating triglycerides, and ALAT, which are key parameters of metabolic health. Whether 5-HEPE treatment can extend metabolic healthspan or lifespan, particularly in humans, is an exciting avenue that needs further testing.

Conclusions and future perspectives

Here, we report the first comprehensive lipidomic and metabolomic signature in adipose tissue of long-lived mice. Importantly, Ames dwarf mice also have increased thermogenic activity, allowing for a unique perspective of the overlap of aging and thermogenesis. While these types of datasets for adipose tissue have been produced for environmental conditions (e.g., exercise), these types of insights have yet to be produced in the context of aging. The data we present here adds to the growing body of literature that suggests lipid metabolism is critical to metabolic aging, and potentially lifespan. Importantly, we extend this knowledge to also include oxylipins and demonstrate that 5-HEPE is potentially a lipid that can beneficially impact metabolism. Together, our data helps to pave a new avenue of lipid research as it pertains to healthy aging.

References

Aguiar-Oliveira MH, Bartke A. Growth hormone deficiency: health and longevity. Endocr Rev. 2019;40:575–601. https://doi.org/10.1210/er.2018-00216.

Andersson A, Sjodin A, Olsson R, Vessby B. Effects of physical exercise on phospholipid fatty acid composition in skeletal muscle. Am J Physiol. 1998;274:E432–8. https://doi.org/10.1152/ajpendo.1998.274.3.E432.

Aon MA, et al. Untangling determinants of enhanced health and lifespan through a multi-omics approach in mice. Cell Metab. 2020. https://doi.org/10.1016/j.cmet.2020.04.018.

Ayyadevara S, et al. Aspirin inhibits oxidant stress, reduces age-associated functional declines, and extends lifespan of Caenorhabditis elegans. Antioxid Redox Signal. 2013;18: 481–90. https://doi.org/10.1089/ars.2011.4151.

Blackburn GL, Walker WA. Science-based solutions to obesity: what are the roles of academia, government, industry, and health care? Am J Clin Nutr. 2005;82:207S–10S. https://doi.org/10.1093/ajcn/82.1.207S.

Brown-Borg HM, Rakoczy SG. Growth hormone administration to long-living dwarf mice alters multiple components of the antioxidative defense system. Mech Ageing Dev. 2003;124: 1013–24. https://doi.org/10.1016/j.mad.2003.07.001.

Brown-Borg HM, Borg KE, Meliska CJ, Bartke A. Dwarf mice and the ageing process. Nature. 1996;384:33. https://doi.org/10.1038/384033a0.

Chaurasia B, Kaddai VA, Lancaster GI, Henstridge DC, Sriram S, Galam DLA, et al. Adipocyte ceramides regulate subcutaneous adipose browning, inflammation, and metabolism. Cell Metab. 2016;24:820–34. https://doi.org/10.1016/j.cmet.2016.10.002.

Chavez JA, Summers SA. A ceramide-centric view of insulin resistance. Cell Metab. 2012;15:585–94. https://doi.org/10.1016/j.cmet.2012.04.002.

Chen KY, Brychta RJ, Abdul Sater Z, Cassimatis TM, Cero C, Fletcher LA, et al. Opportunities and challenges in the therapeutic activation of human energy expenditure and thermogenesis to manage obesity. J Biol Chem. 2019;295:1926–42. https://doi.org/10.1074/jbc.REV119.007363.

Cheng S, Wiklund P, Autio R, Borra R, Ojanen X, Xu L, et al. Adipose tissue dysfunction and altered systemic amino acid metabolism are associated with non-alcoholic fatty liver disease. PLoS One. 2015;10:e0138889. https://doi.org/10.1371/journal.pone.0138889.

Cutler RG, Thompson KW, Camandola S, Mack KT, Mattson MP. Sphingolipid metabolism regulates development and lifespan in Caenorhabditis elegans. Mech Ageing Dev. 2014;143-144:9–18. https://doi.org/10.1016/j.mad.2014.11.002.

Cypess AM, et al. Identification and importance of brown adipose tissue in adult humans. N Engl J Med. 2009;360:1509–17. https://doi.org/10.1056/NEJMoa0810780.

Darcy J, Bartke A. Functionally enhanced brown adipose tissue in Ames dwarf mice. Adipocyte. 2017;6:62–7. https://doi.org/10.1080/21623945.2016.1274470.

Darcy J, Tseng YH. ComBATing aging-does increased brown adipose tissue activity confer longevity? Geroscience. 2019;41:285–96. https://doi.org/10.1007/s11357-019-00076-0.

Darcy J, McFadden S, Fang Y, Huber JA, Zhang C, Sun LY, et al. Brown adipose tissue function is enhanced in long-lived, male Ames dwarf mice. Endocrinology. 2016;157:4744–53. https://doi.org/10.1210/en.2016-1593.

Darcy J, McFadden S, Bartke A. Altered structure and function of adipose tissue in long-lived mice with growth hormone-related mutations. Adipocyte. 2017;6:69–75. https://doi.org/10.1080/21623945.2017.1308990.

Darcy J, McFadden S, Fang Y, Berryman DE, List EO, Milcik N, et al. Increased environmental temperature normalizes energy metabolism outputs between normal and Ames dwarf mice. Aging (Albany NY). 2018;10:2709–22. https://doi.org/10.18632/aging.101582.

Delic V, Griffin JWD, Zivkovic S, Zhang Y, Phan TA, Gong H, et al. Individual amino acid supplementation can improve energy metabolism and decrease ROS production in neuronal cells overexpressing alpha-synuclein. Neuromolecular Med. 2017;19:322–44. https://doi.org/10.1007/s12017-017-8448-8.

Duan J, et al. Dietary supplementation with L-glutamate and L-aspartate alleviates oxidative stress in weaned piglets challenged with hydrogen peroxide. Amino Acids. 2016;48:53–64. https://doi.org/10.1007/s00726-015-2065-3.

Goldman DP, Cutler D, Rowe JW, Michaud PC, Sullivan J, Peneva D, et al. Substantial health and economic returns from delayed aging may warrant a new focus for medical research. Health Aff (Millwood). 2013;32:1698–705. https://doi.org/10.1377/hlthaff.2013.0052.

Gonzalez-Covarrubias V, et al. Lipidomics of familial longevity. Aging Cell. 2013;12:426–34. https://doi.org/10.1111/acel.12064.

Goto-Inoue N, Yamada K, Inagaki A, Furuichi Y, Ogino S, Manabe Y, et al. Lipidomics analysis revealed the phospholipid compositional changes in muscle by chronic exercise and high-fat diet. Sci Rep. 2013;3:3267. https://doi.org/10.1038/srep03267.

Green CL, et al. The effects of graded levels of calorie restriction: IX. Global metabolomic screen reveals modulation of carnitines, sphingolipids and bile acids in the liver of C57BL/6 mice. Aging Cell. 2017;16:529–40. https://doi.org/10.1111/acel.12570.

Green CL, et al. The effects of graded levels of calorie restriction: XIV. Global metabolomics screen reveals brown adipose tissue changes in amino acids, catecholamines, and antioxidants after short-term restriction in C57BL/6 mice. J Gerontol A Biol Sci Med Sci. 2020;75:218–29. https://doi.org/10.1093/gerona/glz023.

Helms SA, Azhar G, Zuo C, Theus SA, Bartke A, Wei JY. Smaller cardiac cell size and reduced extra-cellular collagen might be beneficial for hearts of Ames dwarf mice. Int J Biol Sci. 2010;6:475–90. https://doi.org/10.7150/ijbs.6.475.

Hill CM, Fang Y, Miquet JG, Sun LY, Masternak MM, Bartke A. Long-lived hypopituitary Ames dwarf mice are resistant to the detrimental effects of high-fat diet on metabolic function and energy expenditure. Aging Cell. 2016;15:509–21. https://doi.org/10.1111/acel.12467.

Hoene M, Li J, Haring HU, Weigert C, Xu G, Lehmann R. The lipid profile of brown adipose tissue is sex-specific in mice. Biochim Biophys Acta. 2014;1842:1563–70. https://doi.org/10.1016/j.bbalip.2014.08.003.

Hoffman JM, Poonawalla A, Icyuz M, Swindell WR, Wilson L, Barnes S, et al. Transcriptomic and metabolomic profiling of long-lived growth hormone releasing hormone knock-out mice: evidence for altered mitochondrial function and amino acid metabolism. Aging (Albany NY). 2020;12. https://doi.org/10.18632/aging.102822.

Huang X, Withers BR, Dickson RC. Sphingolipids and lifespan regulation. Biochim Biophys Acta. 2014;1841:657–64. https://doi.org/10.1016/j.bbalip.2013.08.006.

Hulbert AJ, Faulks SC, Buffenstein R. Oxidation-resistant membrane phospholipids can explain longevity differences among the longest-living rodents and similarly-sized mice. J Gerontol A Biol Sci Med Sci. 2006a;61:1009–18. https://doi.org/10.1093/gerona/61.10.1009.

Hulbert AJ, Faulks SC, Harper JM, Miller RA, Buffenstein R. Extended longevity of wild-derived mice is associated with peroxidation-resistant membranes. Mech Ageing Dev. 2006b;127:653–7. https://doi.org/10.1016/j.mad.2006.03.002.

Ikeda K, Maretich P, Kajimura S. The common and distinct features of brown and beige adipocytes. Trends Endocrinol Metab. 2018;29:191–200. https://doi.org/10.1016/j.tem.2018.01.001.

Iwasa M, et al. Elevation of branched-chain amino acid levels in diabetes and NAFL and changes with antidiabetic drug treatment. Obes Res Clin Pract. 2015;9:293–7. https://doi.org/10.1016/j.orcp.2015.01.003.

Joshi AS, Zhou J, Gohil VM, Chen S, Greenberg ML. Cellular functions of cardiolipin in yeast. Biochim Biophys Acta. 2009;1793:212–8. https://doi.org/10.1016/j.bbamcr.2008.07.024.

Kajimura S, Spiegelman BM, Seale P. Brown and beige fat: physiological roles beyond heat generation. Cell Metab. 2015;22:546–59. https://doi.org/10.1016/j.cmet.2015.09.007.

Khosla S, Farr JN, Tchkonia T, Kirkland JL. The role of cellular senescence in ageing and endocrine disease. Nat Rev Endocrinol. 2020. https://doi.org/10.1038/s41574-020-0335-y.

Kirkland JL. Translating the science of aging into therapeutic interventions. Cold Spring Harb Perspect Med. 2016;6: a025908. https://doi.org/10.1101/cshperspect.a025908.

Kogure R, Toyama K, Hiyamuta S, Kojima I, Takeda S. 5-Hydroxy-eicosapentaenoic acid is an endogenous GPR119 agonist and enhances glucose-dependent insulin secretion. Biochem Biophys Res Commun. 2011;416:58–63. https://doi.org/10.1016/j.bbrc.2011.10.141.

Leiria LO, et al. 12-Lipoxygenase regulates cold adaptation and glucose metabolism by producing the omega-3 lipid 12-HEPE from brown fat. Cell Metab. 2019;30:768–783 e767. https://doi.org/10.1016/j.cmet.2019.07.001.

Lewis KN, Rubinstein ND, Buffenstein R. A window into extreme longevity; the circulating metabolomic signature of the naked mole-rat, a mammal that shows negligible senescence. Geroscience. 2018;40:105–21. https://doi.org/10.1007/s11357-018-0014-2.

Lu X, Solmonson A, Lodi A, Nowinski SM, Sentandreu E, Riley CL, et al. The early metabolomic response of adipose tissue during acute cold exposure in mice. Sci Rep. 2017;7:3455. https://doi.org/10.1038/s41598-017-03108-x.

Lynes MD, Tseng YH. Deciphering adipose tissue heterogeneity. Ann N Y Acad Sci. 2018;1411:5–20. https://doi.org/10.1111/nyas.13398.

Lynes MD, et al. The cold-induced lipokine 12,13-diHOME promotes fatty acid transport into brown adipose tissue. Nat Med. 2017;23:631–7. https://doi.org/10.1038/nm.4297.

Lynes MD, Shamsi F, Sustarsic EG, Leiria LO, Wang CH, Su SC, et al. Cold-activated lipid dynamics in adipose tissue highlights a role for cardiolipin in thermogenic metabolism. Cell Rep. 2018;24:781–90. https://doi.org/10.1016/j.celrep.2018.06.073.

Lynes MD, Kodani SD, Tseng YH. Lipokines and thermogenesis. Endocrinology. 2019;160:2314–25. https://doi.org/10.1210/en.2019-00337.

Mancuso P, Bouchard B. The impact of aging on adipose function and adipokine synthesis. Front Endocrinol (Lausanne). 2019;10:137. https://doi.org/10.3389/fendo.2019.00137.

Masternak MM, Bartke A. Growth hormone, inflammation and aging. Pathobiol Aging Age Relat Dis. 2012;2. https://doi.org/10.3402/pba.v2i0.17293.

May FJ, Baer LA, Lehnig AC, So K, Chen EY, Gao F, et al. Lipidomic adaptations in white and brown adipose tissue in response to exercise demonstrate molecular species-specific remodeling. Cell Rep. 2017;18:1558–72. https://doi.org/10.1016/j.celrep.2017.01.038.

Nagahora N, Yamada H, Kikuchi S, Hakozaki M, Yano A. Nrf2 activation by 5-lipoxygenase metabolites in human umbilical vascular endothelial cells nutrients. 2017;9. https://doi.org/10.3390/nu9091001.

Nedergaard J, Cannon B. The changed metabolic world with human brown adipose tissue: therapeutic visions. Cell Metab. 2010;11:268–72. https://doi.org/10.1016/j.cmet.2010.03.007.

Nedergaard J, Bengtsson T, Cannon B. Unexpected evidence for active brown adipose tissue in adult humans. Am J Physiol Endocrinol Metab. 2007;293:E444–52. https://doi.org/10.1152/ajpendo.00691.2006.

Newgard CB, et al. A branched-chain amino acid-related metabolic signature that differentiates obese and lean humans and contributes to insulin resistance. Cell Metab. 2009;9:311–26. https://doi.org/10.1016/j.cmet.2009.02.002.

Ni H, Lu L, Deng J, Fan W, Li T, Yao J. Effects of glutamate and aspartate on serum antioxidative enzyme, sex hormones, and genital inflammation in boars challenged with hydrogen peroxide mediators. Inflamm. 2016;10:4394695. https://doi.org/10.1155/2016/4394695.

Oguri Y, Kajimura S. Cellular heterogeneity in brown adipose tissue. J Clin Invest. 2020;130:65–7. https://doi.org/10.1172/JCI133786.

Oh SI, Lee MS, Kim CI, Song KY, Park SC. Aspartate modulates the ethanol-induced oxidative stress and glutathione utilizing enzymes in rat testes. Exp Mol Med. 2002;34:47–52. https://doi.org/10.1038/emm.2002.7.

Onodera T, Fukuhara A, Shin J, Hayakawa T, Otsuki M, Shimomura I. Eicosapentaenoic acid and 5-HEPE enhance macrophage-mediated Treg induction in mice. Sci Rep. 2017;7:4560. https://doi.org/10.1038/s41598-017-04474-2.

Paradies G, Petrosillo G, Paradies V, Ruggiero FM. Oxidative stress, mitochondrial bioenergetics, and cardiolipin in aging. Free Radic Biol Med. 2010;48:1286–95. https://doi.org/10.1016/j.freeradbiomed.2010.02.020.

Pietrocola F, Castoldi F, Markaki M, Lachkar S, Chen G, Enot DP, et al. Aspirin recapitulates features of caloric restriction. Cell Rep. 2018;22:2395–407. https://doi.org/10.1016/j.celrep.2018.02.024.

Ramstedt U, Serhan CN, Lundberg U, Wigzell H, Samuelsson B. Inhibition of human natural killer cell activity by (14R,15S)-14,15-dihydroxy-5Z,8Z,10E,12E- icosatetraenoic acid. Proc Natl Acad Sci U S A. 1984;81:6914–8. https://doi.org/10.1073/pnas.81.22.6914.

Rattray NJW, Trivedi DK, Xu Y, Chandola T, Johnson CH, Marshall AD, et al. Metabolic dysregulation in vitamin E and carnitine shuttle energy mechanisms associate with human frailty. Nat Commun. 2019;10:5027. https://doi.org/10.1038/s41467-019-12716-2.

Reckelhoff JF, Kellum JA Jr, Racusen LC, Hildebrandt DA. Long-term dietary supplementation with L-arginine prevents age-related reduction in renal function. Am J Physiol. 1997;272:R1768–74. https://doi.org/10.1152/ajpregu.1997.272.6.R1768.

Rojanathammanee L, Rakoczy S, Brown-Borg HM. Growth hormone alters the glutathione S-transferase and mitochondrial thioredoxin systems in long-living Ames dwarf mice. J Gerontol A Biol Sci Med Sci. 2014;69:1199–211. https://doi.org/10.1093/gerona/glt178.

Romanick MA, Rakoczy SG, Brown-Borg HM. Long-lived Ames dwarf mouse exhibits increased antioxidant defense in skeletal muscle. Mech Ageing Dev. 2004;125:269–81. https://doi.org/10.1016/j.mad.2004.02.001.

Saito M, et al. High incidence of metabolically active brown adipose tissue in healthy adult humans: effects of cold exposure and adiposity. Diabetes. 2009;58:1526–31. https://doi.org/10.2337/db09-0530.

Schrauwen P, van Marken Lichtenbelt WD, Spiegelman BM. The future of brown adipose tissues in the treatment of type 2 diabetes. Diabetologia. 2015;58:1704–7. https://doi.org/10.1007/s00125-015-3611-y.

Schulz TJ, et al. Brown-fat paucity due to impaired BMP signalling induces compensatory browning of white fat. Nature. 2013;495:379–83. https://doi.org/10.1038/nature11943.

Serhan CN, Levy BD. Resolvins in inflammation: emergence of the pro-resolving superfamily of mediators. J Clin Invest. 2018;128:2657–69. https://doi.org/10.1172/JCI97943.

Sharma S, Rakoczy S, Dahlheimer K, Brown-Borg H. The hippocampus of Ames dwarf mice exhibits enhanced antioxidative defenses following kainic acid-induced oxidative stress. Exp Gerontol. 2010;45:936–49. https://doi.org/10.1016/j.exger.2010.08.013.

Simcox J, et al. Global analysis of plasma lipids identifies liver-derived acylcarnitines as a fuel source for brown fat thermogenesis. Cell Metab. 2017;26:509–522 e506. https://doi.org/10.1016/j.cmet.2017.08.006.

Spite M, Claria J, Serhan CN. Resolvins, specialized proresolving lipid mediators, and their potential roles in metabolic diseases. Cell Metab. 2014;19:21–36. https://doi.org/10.1016/j.cmet.2013.10.006.

Stanford KI, et al. A novel role for subcutaneous adipose tissue in exercise-induced improvements in glucose homeostasis. Diabetes. 2015;64:2002–14. https://doi.org/10.2337/db14-0704.

Stout MB, et al. Growth hormone action predicts age-related white adipose tissue dysfunction and senescent cell burden in mice.

Aging (Albany NY). 2014;6:575–86. https://doi.org/10.18632/aging.100681.

Strong R, et al. Nordihydroguaiaretic acid and aspirin increase lifespan of genetically heterogeneous male mice. Aging Cell. 2008;7:641–50. https://doi.org/10.1111/j.1474-9726.2008.00414.x.

Strong R, et al. Longer lifespan in male mice treated with a weakly estrogenic agonist, an antioxidant, an alpha-glucosidase inhibitor or a Nrf2-inducer. Aging Cell. 2016;15:872–84. https://doi.org/10.1111/acel.12496.

Sustarsic EG, et al. Cardiolipin synthesis in brown and beige fat mitochondria is essential for systemic energy homeostasis. Cell Metab. 2018;28:159–174 e111. https://doi.org/10.1016/j.cmet.2018.05.003.

Sverdlov AL, Ngo DT, Chan WP, Chirkov YY, Horowitz JD. Aging of the nitric oxide system: are we as old as our NO? J Am Heart Assoc. 2014;3. https://doi.org/10.1161/JAHA.114.000973.

Tolstikov V, Nikolayev A, Dong S, Zhao G, Kuo MS. Metabolomics analysis of metabolic effects of nicotinamide phosphoribosyltransferase (NAMPT) inhibition on human cancer cells. PLoS One. 2014;9:e114019. https://doi.org/10.1371/journal.pone.0114019.

Ussher JR, et al. Inhibition of de novo ceramide synthesis reverses diet-induced insulin resistance and enhances whole-body oxygen consumption. Diabetes. 2010;59:2453–64. https://doi.org/10.2337/db09-1293.

Valencak TG, Ruf T. Phospholipid composition and longevity: lessons from Ames dwarf mice. Age (Dordr). 2013;35:2303–13. https://doi.org/10.1007/s11357-013-9533-z.

van Marken Lichtenbelt WD, et al. Cold-activated brown adipose tissue in healthy men. N Engl J Med. 2009;360:1500–8. https://doi.org/10.1056/NEJMoa0808718.

Villarroya F, Cereijo R, Villarroya J, Giralt M. Brown adipose tissue as a secretory organ. Nat Rev Endocrinol. 2017;13:26–35. https://doi.org/10.1038/nrendo.2016.136.

Viltard M, et al. The metabolomic signature of extreme longevity: naked mole rats versus mice. Aging (Albany NY). 2019;11:4783–800. https://doi.org/10.18632/aging.102116.

Virtanen KA, et al. Functional brown adipose tissue in healthy adults. N Engl J Med. 2009;360:1518–25. https://doi.org/10.1056/NEJMoa0808949.

Wan QL, Zheng SQ, Wu GS, Luo HR. Aspirin extends the lifespan of Caenorhabditis elegans via AMPK and DAF-16/FOXO in dietary restriction pathway. Exp Gerontol. 2013;48:499–506. https://doi.org/10.1016/j.exger.2013.02.020.

Wang Z, Al-Regaiey KA, Masternak MM, Bartke A. Adipocytokines and lipid levels in Ames dwarf and calorie-restricted mice. J Gerontol A Biol Sci Med Sci. 2006;61:323–31. https://doi.org/10.1093/gerona/61.4.323.

Wang C, et al. Hydroxyeicosapentaenoic acids and epoxyeicosatetraenoic acids attenuate early occurrence of nonalcoholic fatty liver disease. Br J Pharmacol. 2017;174:2358–72. https://doi.org/10.1111/bph.13844.

Westbrook R, Bonkowski MS, Strader AD, Bartke A. Alterations in oxygen consumption, respiratory quotient, and heat production in long-lived GHRKO and Ames dwarf mice, and short-lived bGH transgenic mice. J Gerontol A Biol Sci Med Sci. 2009;64:443–51. https://doi.org/10.1093/gerona/gln075.

Westbrook R, Bonkowski MS, Arum O, Strader AD, Bartke A. Metabolic alterations due to caloric restriction and every other day feeding in normal and growth hormone receptor knockout mice. J Gerontol A Biol Sci Med Sci. 2014;69:25–33. https://doi.org/10.1093/gerona/glt080.

Wiesenborn DS, Ayala JE, King E, Masternak MM. Insulin sensitivity in long-living Ames dwarf mice. Age (Dordr). 2014;36:9709. https://doi.org/10.1007/s11357-014-9709-1.

Yang Q, Vijayakumar A, Kahn BB. Metabolites as regulators of insulin sensitivity and metabolism. Nat Rev Mol Cell Biol. 2018;19:654–72. https://doi.org/10.1038/s41580-018-0044-8.

Yoneshiro T, et al. BCAA catabolism in brown fat controls energy homeostasis through SLC25A44. Nature. 2019;572:614–9. https://doi.org/10.1038/s41586-019-1503-x.

Yore MM, et al. Discovery of a class of endogenous mammalian lipids with anti-diabetic and anti-inflammatory effects. Cell. 2014;159:318–32. https://doi.org/10.1016/j.cell.2014.09.035.

Zhu Y, Armstrong JL, Tchkonia T, Kirkland JL. Cellular senescence and the senescent secretory phenotype in age-related chronic diseases. Curr Opin Clin Nutr Metab Care. 2014;17:324–8. https://doi.org/10.1097/MCO.0000000000000065.

Zingaretti MC, et al. The presence of UCP1 demonstrates that metabolically active adipose tissue in the neck of adult humans truly represents brown adipose tissue. FASEB J. 2009;23:3113–20. https://doi.org/10.1096/fj.09-133546.